the plant journal

SEB SOCIETY FOR EXPERIMENTAL BIOLOGY

The Plant Journal (2025) **121,** e17169 doi: 10.1111/tpj.17169

Gene family rearrangements and transcriptional priming drive the evolution of vegetative desiccation tolerance in *Selaginella*

Gerardo Alejo-Jacuinde[1], Ricardo A. Chávez Montes[1], Cristian D. Gutierrez Reyes[2], Lenin Yong-Villalobos[1], June Simpson[3] and Luis Herrera-Estrella[1,4,*]

[1]*Department of Plant and Soil Science, Institute of Genomics for Crop Abiotic Stress Tolerance (IGCAST), Texas Tech University, Lubbock, Texas 79409, USA,*

[2]*Department of Chemistry and Biochemistry, Texas Tech University, Lubbock, Texas 79409, USA,*

[3]*Department of Genetic Engineering, Centro de Investigación y de Estudios Avanzados del Instituto Politécnico Nacional, 36824 Irapuato, Guanajuato, Mexico, and*

[4]*Unidad de Genómica Avanzada/Langebio, Centro de Investigación y de Estudios Avanzados del Instituto Politécnico Nacional, Gto. 36824, Irapuato, Mexico*

Received 14 August 2024; revised 11 November 2024; accepted 13 November 2024; published online 12 December 2024.
*For correspondence (e-mail luis.herrera-estrella@ttu.edu).

SUMMARY

Extreme dryness is lethal for nearly all plants, excluding the so-called resurrection plants, which evolved vegetative desiccation tolerance (VDT) by recruiting genes common in most plants. To better understand the evolution of VDT, we generated chromosome-level assemblies and improved genome annotations of two *Selaginella* species with contrasting abilities to survive desiccation. We identified genomic features and critical mechanisms associated with VDT through sister-group comparative genomics integrating multi-omics data. Our findings indicate that *Selaginella* evolved VDT through the expansion of some stress protection-related gene families and the contraction of senescence-related genes. Comparative analyses revealed that desiccation-tolerant *Selaginella* species employ a combination of constitutive and inducible protection mechanisms to survive desiccation. We show that transcriptional priming of stress tolerance-related genes and accumulation of flavonoids in unstressed plants are hallmarks of VDT in *Selaginella*. During water loss, the resurrection *Selaginella* induces phospholipids and glutathione metabolism, responses that are missing in the desiccation-sensitive species. Additionally, gene regulatory network analyses indicate the suppression of growth processes as a major component of VDT. This study presents novel perspectives on how gene dosage impacts crucial protective mechanisms and the regulation of central processes to survive extreme dehydration.

Keywords: comparative genomics, inducible protection mechanisms, metabolomics, priming, *Selaginella*, transcriptomic, vegetative desiccation tolerance.

INTRODUCTION

During the evolution of land plants, vegetative desiccation tolerance (VDT) arose as an adaptation to survive the fluctuations in water availability in terrestrial environments. Thus, VDT represented an essential feature for the colonization of terrestrial environments by primitive plants from a freshwater origin (Oliver et al., 2000). Later, plants evolved into more morphologically complex systems, and desiccation tolerance (DT) was lost in vegetative tissues and confined to reproductive structures in the early evolution of tracheophytes (Alpert & Oliver, 2002; Oliver et al., 2000). Vascular plant species exhibiting VDT belong to diverse plant lineages that evolved this trait independently (Marks et al., 2021). For this reason, some plant adaptations to dry environments, including VDT, have been previously described as convergent evolutive events (Artur & Kajala, 2021).

Different lineages of resurrection species display common VDT mechanisms, including carbohydrate accumulation, synthesis of compatible solutes, increased antioxidant activity, and induction of stress-associated proteins, among others (Farrant et al., 2007; Gechev et al., 2021; Oliver et al., 2020). However, there is no unique strategy to survive desiccation, and VDT can be considered a

highly diverse and variable phenomenon. Plants that survive rapid water loss, such as desiccation-tolerant bryophytes, possess a constitutively active protection strategy (Proctor et al., 2007). In contrast, other plants require a gradual water loss to induce protection mechanisms, as observed in resurrection angiosperms (Giarola et al., 2017). Moreover, ferns and lycophytes exhibit an intermediate VDT strategy combining inducible and constitutive protection mechanisms (Alejo-Jacuinde & Herrera-Estrella, 2022). Current knowledge indicates that the ability to survive desiccation implies a combination of shared protection mechanisms and species-specific responses. Indeed, some of the protection mechanisms activated in resurrection species represent common responses to water loss observed in sensitive plants. In most plants, water loss triggers responses to prevent cellular damage, including the production of stress-protectant metabolites (e.g., proline), antioxidant enzymes (e.g., peroxidases), and activation of the abscisic acid (ABA) signaling pathway (Gupta et al., 2020; Osakabe et al., 2014). However, several unresolved questions regarding key differences in the molecular response between drought and desiccation exist. An important difference between desiccation-tolerant and sensitive plants could be the level or kinetics of activation of these protection mechanisms. For instance, the expansion of the early light-inducible proteins (ELIPs) gene family in the genomes of resurrection species appears as an important feature for the evolution of VDT (VanBuren et al., 2019). A higher dosage of genes encoding ELIPs in some resurrection genomes leads to a higher combined expression during water stress compared to closely related sensitive species (Chávez Montes et al., 2022). Considering that most of the genes involved in the protection mechanisms activated in resurrection plants are also present in desiccation-sensitive species (Costa, Artur, et al., 2017; Giarola et al., 2017; Hilhorst et al., 2018), a central question in DT research is how resurrection species activate VDT-expressing gene families present in all plants.

Comparative analyses using phylogenetically related species that differ in their ability to tolerate desiccation represent an excellent approach to identifying the molecular basis of VDT. Among resurrection lineages, the *Selaginella* genus is an ideal model system that includes closely related desiccation-tolerant and sensitive species, allowing suitable sister group comparisons. Here, we report the assembly of the genomes of *Selaginella sellowii* (desiccation tolerant) and *Selaginella silvestris* (desiccation sensitive) to a chromosome-scale level. Sister group comparisons at critical stages during water loss allowed the identification of key responses and protection mechanisms in the resurrection species that are absent in the desiccation-sensitive species. Several differential responses between desiccation-tolerant and desiccation-sensitive *Selaginella* correspond to gene family rearrangements. These findings strongly correlate with transcriptomic, lipidomic, and metabolomic data, such as significant differences in phospholipid and glutathione metabolism. Additionally, gene regulatory network analyses identified several transcription factors (TFs) with a central role as regulators during VDT. In general, VDT in *Selaginella* involves a complex regulation to activate protection mechanisms and downregulate specific processes to successfully adapt to extreme water loss.

RESULTS

Genome sequencing and chromosome-level genome assemblies

The closely related species *S. silvestris* (sensitive) and *S. sellowii* (tolerant) were selected for their contrasting abilities to survive desiccation in their vegetative tissues (Figure 1; Video S1). For genome sequencing, DNA was isolated from *S. silvestris* and *S. sellowii* individuals that were previously clonally propagated under laboratory conditions (Figure 1a). Genome heterozygosity for each species was calculated by *k*-mer frequency distribution. The level of heterozygosity was approximately 0.79% and 0.42% for *S. silvestris* and *S. sellowii*, respectively (Figure S2). A total of seven distinct pipelines using different assembly algorithms were evaluated to select the best strategy to reconstruct *Selaginella* genomes. Results of these analyses indicated that the MaSuRCA pipeline (Zimin et al., 2017), which combines PacBio and Illumina reads, produced the most contiguous and complete genome assemblies for both *Selaginella* species. The following steps to generate the genome reference for *S. silvestris* and *S. sellowii* differed. Method S1 contains a detailed description of the procedures performed for each *Selaginella* species. The final *Selaginella* genomes showed high genome contiguity with a scaffold N50 of 5.63 and 5.89 Mb for *S. silvestris* and *S. sellowii*, respectively (Figure 1b). The genome GC content was calculated at 50.18% and 49.65% for *S. silvestris* and *S. sellowii*, respectively, similar to the 49.59% GC content of their close relative *S. lepidophylla*. The two *Selaginella* genome assemblies were organized into ten pseudo-chromosomes ranging from 8.22 to 4.56 Mb, showing high collinearity between the two species (Figure 1c). The genomes generated in this study significantly improved the proportion of complete and single-copy BUSCOs compared to other available *Selaginella* genomes (Figure S3). Contrary to previous studies in *Selaginella*, the genome of the desiccation-sensitive *S. silvestris* exhibited a slightly higher proportion of repetitive sequences than the desiccation-tolerant *S. sellowii* (41.19% and 38.89%, respectively). In both *Selaginella* species, most of these repetitive sequences were annotated as long terminal repeat (LTR) retrotransposons. Among LTR retrotransposons, Gypsy elements were the most predominant

(a)

(b)

Assembly metrics	*S. silvestris*	*S. sellowii*
Total length (bp)	74,033,417	72,147,376
Sequences	646	685
Sequences ≥50 kbp	27	24
GC content (%)	50.18%	49.65%
Scaffold N50 (bp)	5,632,811	5,894,053
Scaffold L50	6	6
Largest scaffold (bp)	7,934,426	8,227,566
Annotated genes	19,063	17,406
Gene average size	1,799.8 bp	1,896.2 bp

(c)

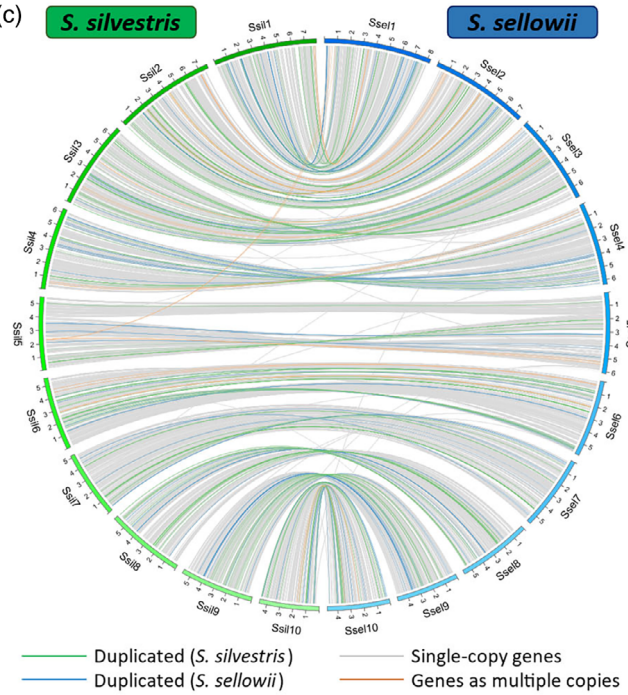

(d)

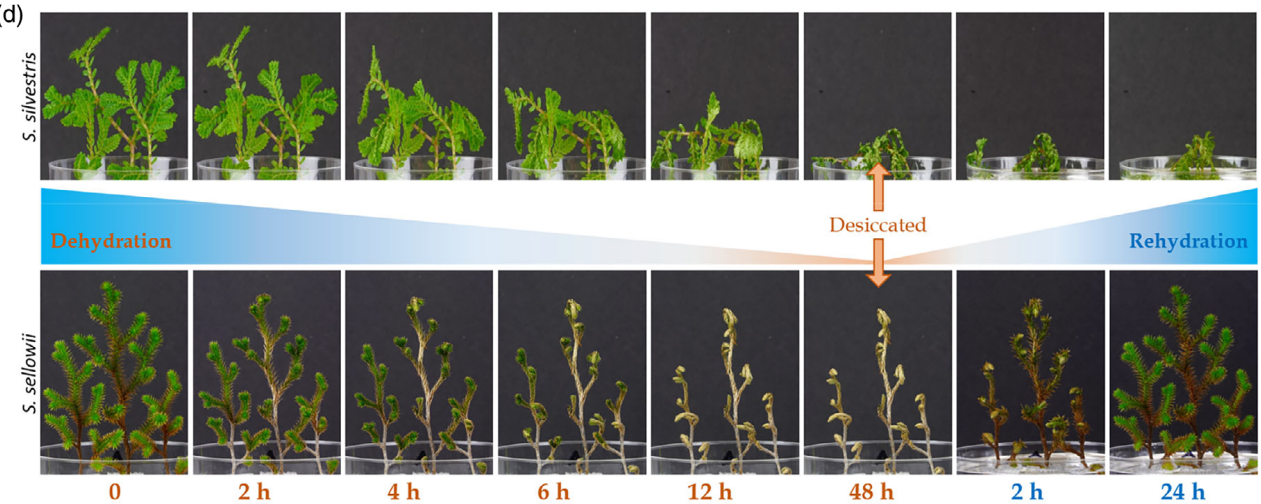

Figure 1. Strong similarity between *Selaginella* genomes and contrasting ability to survive desiccation.
(a) Photographs showing morphological differences between desiccation-sensitive *S. silvestris* and desiccation-tolerant *S. sellowii*.
(b) Assembly metrics for the *Selaginella* genomes generated in the present study.
(c) Macrosynteny showing high collinearity between the pseudo-chromosomes of *S. silvestris* (green) and *S. sellowii* (blue) using syntenic orthologs (MCScan analysis).
(d) Explants of *S. silvestris* (top) and *S. sellowii* (bottom) exposed to desiccation and subsequent recovery. Photographs at specific intervals during dehydration using MgCl2, and recovery stage at 4 and 12 h after rehydration. The complete dehydration-rehydration cycle is shown in Video S1.

class, spanning 21.55 and 19.95 Mb of *S. silvestris* and *S. sellowii* genomes, respectively.

Selaginella genomes were annotated using the MAKER-P pipeline (Cantarel et al., 2008; Holt & Yandell, 2011b), resulting in 19 063 and 17 406 protein-coding genes for *S. silvestris* and *S. sellowii*, respectively. Predicted protein-coding genes for both species yielded a more complete annotation than previously reported *Selaginella* genomes (Figure 2a). Additionally, annotation edit distance (AED), which is a metric of annotation quality, indicates high congruence between evidence and the predicted gene models: 95.27% and 95.57% of the genes have an AED <0.5 in *S. silvestris* and *S. sellowii*, respectively. Genes in *S. sellowii* had an average length of 1896.2 bp with a mean value of 6.3 exons, whereas the average length in *S. silvestris* was 1799.8 bp with a mean

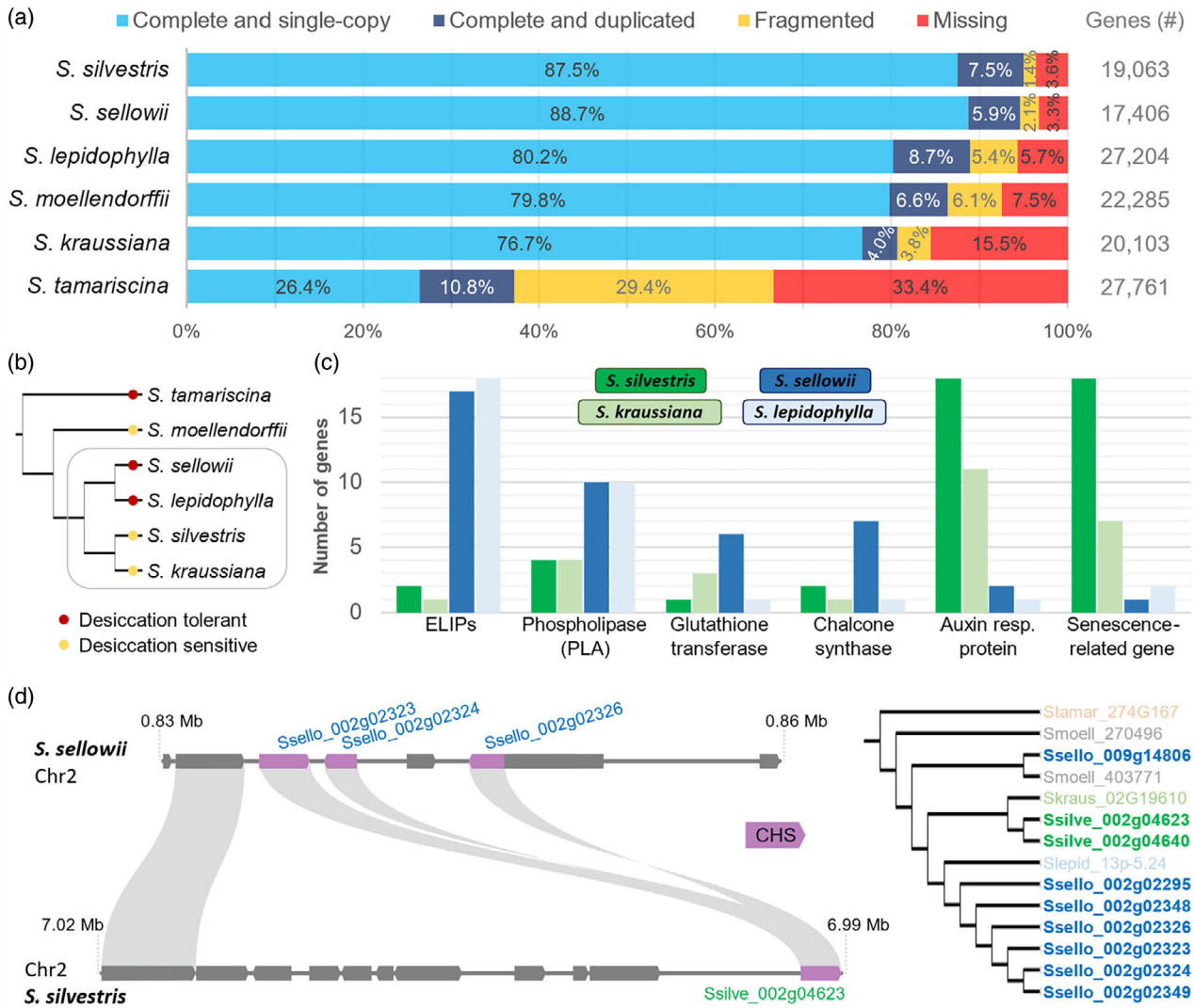

Figure 2. Predicted protein-coding genes and gene family rearrangements in *Selaginella genomes*.
(a) BUSCO analysis showing a significant improvement in structural genome annotation compared to available *Selaginella* genomes (completeness evaluation using viridiplantae dataset).
(b) *Selaginella* species classified as desiccation-tolerant (red dot) or desiccation-sensitive species (yellow dot), along with their phylogenetic relations.
(c) Gene families (orthogroups identified using OrthoFinder) expanded and contracted in resurrection *Selaginella* genomes. This analysis was limited to phylogenetically close relatives that differ in VDT ability; gray rectangle of section (b).
(d) Microsynteny showing tandem repeat duplications of chalcone synthase (CHS) genes. Orthogroup phylogenetic tree indicates species-specific expansion of CHS genes in *S. sellowii* genome compared to other *Selaginella* genomes.

value of 6.1 exons. This difference is also observed in their predicted proteomes, *S. sellowii* possesses slightly larger proteins than the desiccation-sensitive *S. silvestris* (an average of 431.7 compared to 417.6 amino acids, respectively).

Genomic features potentially associated with VDT

Homology analysis using OrthoFinder (Emms & Kelly, 2015) with the protein models of available *Selaginella* genomes (*S. kraussiana*, *S. moellendorffii*, *S. lepidophylla*, *S. tamariscina*) and the species sequenced in this project (*S. silvestris*, *S. sellowii*) yield 20 218 orthogroups representing a total of 133 822 genes. Among them, 5300 orthogroups were present in all *Selaginella* species (Figure S4). To identify gene family expansions and contractions associated with VDT, the analysis was limited to phylogenetically close species that differ in their ability to survive desiccation (Figure 2b). Therefore, this analysis included the desiccation-tolerant *S. sellowii* and *S. lepidophylla*, as well as the desiccation-sensitive *S. silvestris* and *S. kraussiana* (Figure 2c). The orthogroup HOG0314, which includes genes encoding ELIPs, represents the largest expanded gene family in both resurrection *Selaginella* genomes (17–18 copies) compared to desiccation-sensitive species

(1–2 copies). Gene families with phospholipase activity (orthogroup HOG0455; phospholipase A) were also expanded in both desiccation-tolerant *Selaginella* genomes (10 compared to 4 copies). Furthermore, 32 genes with putative phospholipase activity were identified in the genome of desiccation-tolerant *S. sellowii*, whereas only 18 phospholipase genes were identified in the desiccation-sensitive *S. silvestris*. Additional gene families expanded in resurrection *Selaginella* genomes include some protein kinases containing a D-mannose binding lectin (HOG1059; 7–9 compared to 1 copy), lipoxygenase genes (HOG2151; 5–3 compared to 1 copy), and multicopper oxidase genes (HOG0657; 5 compared to 1 copy).

Other gene families were only expanded as a species-specific adaptation in the genome of the desiccation-tolerant *S. sellowii* (Figure 2c). The genome of this species includes seven chalcone/stilbene synthase genes in the orthogroup HOG1700 compared to 1–2 copies in desiccation-sensitive genomes (Figure 2d). Additional gene families expanded in a lower proportion in *S. sellowii* include glutathione transferase genes (HOG0681) and pectinacetylesterase proteins (HOG0369). Compared to desiccation-sensitive species, the resurrection *Selaginella* genomes underwent gene family contractions of some families of auxin-related genes. For instance, the members of the auxin-responsive proteins family in the orthogroup HOG0235 were reduced to only 1–2 members in the desiccation-tolerant species compared to 11–18 copies in the sensitive *Selaginella* genomes. Furthermore, a gene family of senescence-related genes containing 7–18 copies in desiccation-sensitive plants was contracted to only 1–2 copies in desiccation-tolerant species.

Transcriptional priming and constitutive protection mechanisms for VDT

Genes highly expressed under well-watered conditions (100% relative water content, RWC) in each *Selaginella* species were analyzed to identify potential transcriptional priming events associated with VDT. Significantly enriched pathways (GO terms) were identified using the FGSEA method (Korotkevich et al., 2021) and compared between species. The results of this analysis indicated a total of 40 enriched terms shared between the desiccation-sensitive and desiccation-tolerant species. In both *Selaginella* species, the most highly expressed genes in well-watered conditions are involved in mRNA binding, photosynthesis, chloroplast structure, and ribosome-related, among others (Figure 3a). Highly expressed genes in desiccation-tolerant *S. sellowii* under hydrated conditions resulted in 31 GO terms only enriched in this species. Several of these terms are associated with stress responses, indicating transcriptional priming for VDT. Enriched terms specific to the desiccation-tolerant *S. sellowii* included lipid transport and binding, cell wall, lignin biosynthesis, glutathione metabolism, ABA-activated signaling, and defense response. In contrast, the desiccation-sensitive *S. silvestris* displayed gibberellic acid-mediated signaling, cellulose biosynthesis, and peptidase activity, among others.

Additionally, metabolomic analyses indicated that several flavonoids were significantly more abundant in the resurrection *S. sellowii* than the desiccation-sensitive *S. silvestris* (Data S3). The most abundant flavonoids in the desiccation-tolerant *S. sellowii* include apigenin-7-O-beta-D-glucoside, 3′,4′,5,7-tetrahydroxy-3-methoxyflavone, aureusidin 6-O-glucoside, 2′-Hydroxydaidzein, cyanidin3-O-rutinoside, and sophorol. Interestingly, the abundance of several flavonoids in *S. sellowii* is maintained at high levels during water loss, and a few increased their abundance in response to dehydration (Figure 3b). Genes participating in flavonoid biosynthesis pathways were identified in *Selaginella* genomes, and their expression was analyzed. This analysis showed that a set of flavonoid-related genes is highly expressed in the desiccation-tolerant *S. sellowii* in hydrated conditions, which maintain their expression during the entire desiccation treatment (Figure 3c). Among them, four of the most strongly expressed genes encode flavanone 3-dioxygenase or naringenin 3-hydroxylase (EC 1.14.11.9), an enzyme that participates in the early steps of flavonoid biosynthesis (https://www.genome.jp/entry/ec:1.14.11.9). The expression of most flavonoid-related genes in *S. sellowii* is not affected by desiccation, suggesting a constitutive protection strategy to accumulate high levels of flavonoids.

Differentially activated processes during water stress in *Selaginella* species

A differential expression analysis was performed using the package edgeR (Robinson et al., 2010), and the resulting lists of statistically differentially abundant transcripts (SDATs) were assigned to GO biological categories using topGO (Alexa & Rahnenführer, 2007). Most of the genes exhibiting a significant change in transcript level during desiccation treatment are shared between tolerant and sensitive *Selaginella* species, and only 3.59% of the SDATs in *S. sellowii* were members of species-specific orthogroups (Figure S4). These results support the hypothesis that VDT predominantly evolved by recruiting pre-existing plant genes. Under water stress conditions, desiccation-tolerant and desiccation-sensitive *Selaginella* species exhibited similar transcriptional responses (Figure 4). For instance, both species increased the abundance of transcripts involved in the response to ABA and stress (i.e., water deprivation, salt stress, defense response), ethylene-activated signaling pathway, phosphatidylcholine metabolic process, etc. Specifically, this analysis revealed several functional categories related to the VDT phenotype that are not significantly enriched by dehydration in the desiccation-sensitive *S. silvestris*. Significantly enriched

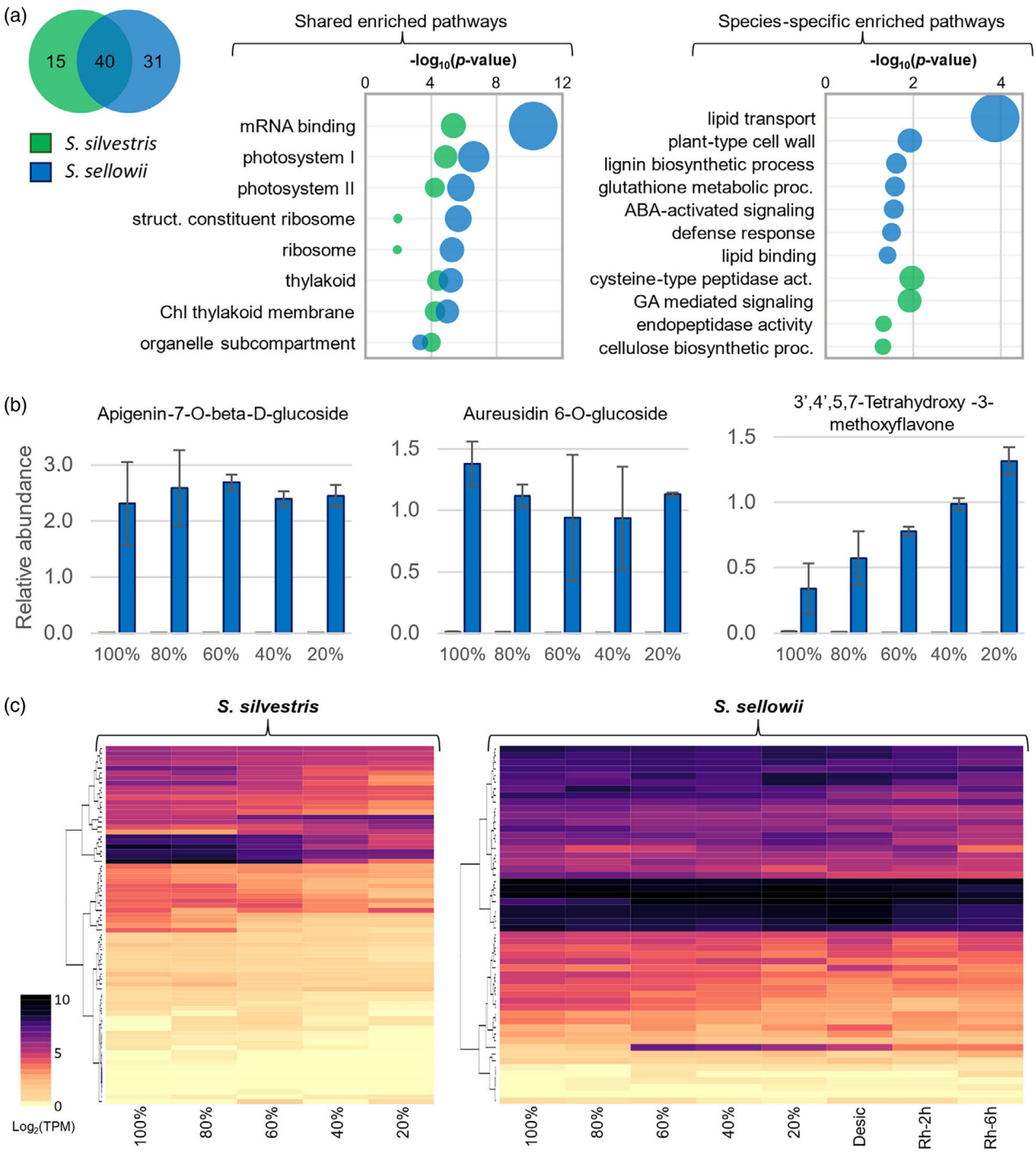

Figure 3. Desiccation-tolerant *S. sellowii* exhibits transcriptional priming and the constitutive accumulation of flavonoids as some strategies for VDT.
(a) Enriched pathways (FGSEA analysis; *P*-value <0.05) of the most expressed genes during hydrated conditions in desiccation-sensitive *S. silvestris* (green) and desiccation-tolerant *S. sellowii* (blue).
(b) Metabolomic analyses indicated flavonoids as some of the most abundant compounds in the resurrection *S. sellowii*. Changes in response to water loss (expressed as RWC) are shown for the three most abundant flavonoids. Each bar represents the average of three technical replicates and error bars indicate the SD.
(c) Expression of genes involved in flavonoid metabolism in the desiccation-sensitive *S. silvestris* (left), and desiccation-tolerant *S. sellowii* (right). Log_2 transformed gene abundance (TPM) during the desiccation process. Desiccation-tolerant species also includes desiccated (Desic) and rehydration (Rh) stages.

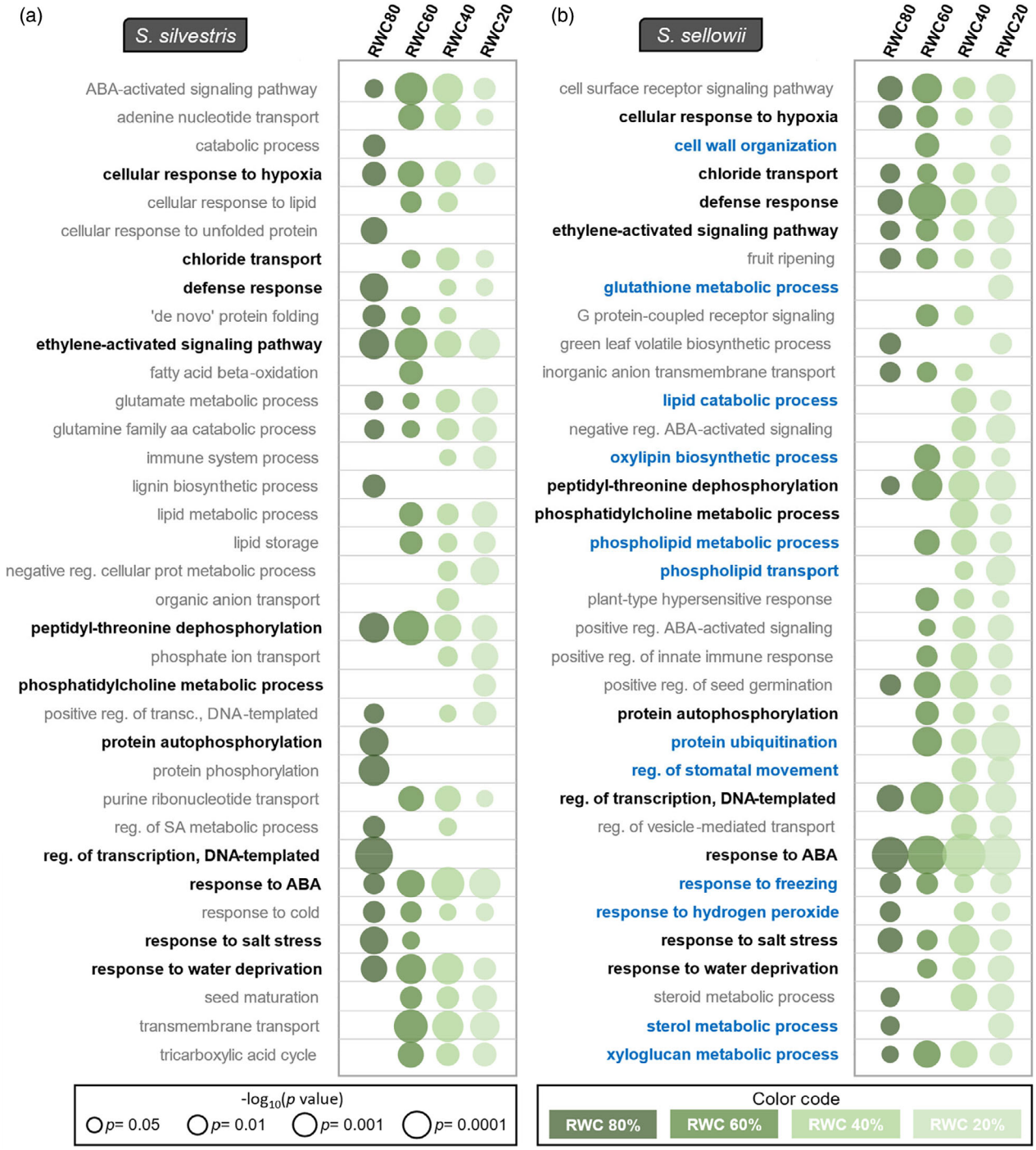

Figure 4. Sister group comparatives indicated key responses associated with VDT in *Selaginella*.
Significantly enriched biological categories at different relative water contents (RWC) during water loss in the desiccation-sensitive *S. silvestris* (a) and the desiccation-tolerant *S. sellowii* (b). Some categories are activated in both *Selaginella* species (bold black) whereas several categories putatively related to VDT phenotype are only observed in the desiccation-tolerant species (blue).

categories only observed in the desiccation-tolerant species included cell wall organization and xyloglucan metabolism, sterol and phospholipid metabolic process, protein ubiquitination, response to hydrogen peroxide and freezing, among others (Figure 4). Additional biological categories, such as response to desiccation and carbohydrate transport, were observed under desiccated conditions and during rehydration in *S. sellowii* (Figure S5).

Below 40% RWC, the desiccation-tolerant *S. sellowii* activated some key responses such as glutathione metabolic process, phospholipid transport, lipid catabolic process, and regulation of stomatal movement. Metabolomic analyses corroborate the activation of some of these key differential transcriptional responses between *Selaginella* species. For instance, desiccation-tolerant *S. sellowii* showed a significant accumulation of glutathione and L-γ-glutamyl amino acids below 40% RWC (Figure S6).

Transcriptome analyses indicated lipid metabolism as an important difference between desiccation-tolerant and desiccation-sensitive *Selaginella* species. In hydrated conditions, *Selaginella* species exhibit distinct abundances in major constituents of plant membranes such as phosphatidylcholines (PC), and monogalactosyldiacylglycerol (MGDG). Both species exhibit the molecule 16:0/18:2-PC as the most abundant PC, whereas 16:3/18:3-MGDG and 18:3/18:3-MGDG were the most abundant MGDG in *S. silvestris* and *S. sellowii*, respectively (Data S2). Both *Selaginella* species increased PC levels and reduced MGDG in response to water loss. Contrasting differences during water stress include a significant increase in lysophosphatidylcholine (LPC), lysophosphatidylethanolamine (LPE), and sterols (St) in the desiccation-tolerant *S. sellowii* (Figure S7), whereas the desiccation-sensitive species showed a decrease of these compounds. At 20% RWC, the relative abundance of LPC and LPE in *S. sellowii* was 5.4 and 4.6 times higher, respectively, than in *S. silvestris*. Additional changes observed in *S. sellowii* in response to water loss included increased abundance of phosphatidylinositol, sphingophospholipids, and wax esters. Although *S. sellowii* showed some SDATs involved in unsaturated fatty acid biosynthesis during desiccation, a detailed analysis of the degree of unsaturation of the fatty acid chains indicated that both *Selaginella* species underwent significant but different changes in the unsaturation profiles during dehydration (Data S3). Among major constituents such as MGDG and PC classes, polyunsaturated molecules that were accumulated in response to dehydration only in the resurrection plant included 18:2/18:2-MGDG, 16:0/18:2-MGDG, and 34:1-PC (Data S2). The abundance of several polyunsaturated species of phosphatidylglycerols (PG) changed in response to dehydration. In the desiccation-tolerant *S. sellowii*, a significant increase was observed in 16:0/18:1-PG and 16:0/18:2-PG, whereas in the desiccation-sensitive species, their abundance was reduced. Furthermore, double bond index analysis indicated that the desiccation-tolerant *S. sellowii* exhibited higher unsaturation in triglycerides (TG) than the desiccation-sensitive *S. silvestris* during dehydration (Data S3). Specific polyunsaturated molecules that significantly increased their abundance in response to dehydration in *S. sellowii* include 18:1/18:2/18:3-TG and 18:2/18:2/18:3-TG.

Identification of central regulators involved in VDT

For the analysis of how resurrection species regulate the activation of VDT mechanisms, gene regulatory networks (GRN) were inferred using the RegEnrich package (Tao et al., 2022). This pipeline provides a gene regulator ranking score, and it was used to identify TFs participating as candidate regulators of VDT. The 15 best-scored regulators per condition during dehydration (and recovery for the resurrection species) were selected for further analysis. Some of these TFs were assigned as central regulators during several stages of the desiccation process, and this selection produced a list of 36 different regulators in both *Selaginella* species (Figure 5). Notably, 31 of the 36 candidate VDT regulators correspond to single-copy syntenic orthologs between the *S. sellowii* and *S. silvestris* genomes. However, only five were assigned as common central regulators to both *Selaginella* species: one member of the CO-like, C2H2, GATA, PLATZ, and Trihelix TF families. Among the candidate regulators of VDT in *S. sellowii*, only one TF has no homologs in the desiccation-sensitive *S. silvestris* (i.e., Ssello002g02436; but has homologs in other *Selaginella* species). The TFs identified as central regulators were functionally annotated using *Arabidopsis thaliana* homologs (Table S1). This analysis indicated various functions, including cell differentiation, development, anatomical-related roles, and response to chemicals and stress. Enrichment analysis of the gene correlations associated with these candidate regulators in the desiccation-tolerant *S. sellowii* indicates several categories related to VDT (i.e., cell wall organization, glutathione transferase activity, lipid metabolism, redox activity). However, the main difference in the regulators' associated network between *Selaginella* species lies in photosynthesis categories (Figure S8). The subnetwork of the resurrection *S. sellowii* was significantly enriched in several photosynthesis-related processes and photosynthetic apparatus modifications, whereas these categories were not enriched in the desiccation-sensitive *S. silvestris*.

Gene expression downregulation as a critical component of VDT

Due to the complexity of the GRNs, which contain 29 206 and 28 430 gene correlations in *S. silvestris* and *S. sellowii*, respectively, the following analyses focused on the previously identified SDATs of each species (Figure S9). The nodes corresponding to SDATs were clustered using self-organizing maps (SOMs). These SDATs were assigned to clusters based on their expression profiles into nine SOMs in each *Selaginella* species (Figures S10 and S11). The average expression of the genes belonging to the same cluster was calculated and used to classify them as upregulated or downregulated clusters. The desiccation-tolerant *S. sellowii* had five upregulated and four

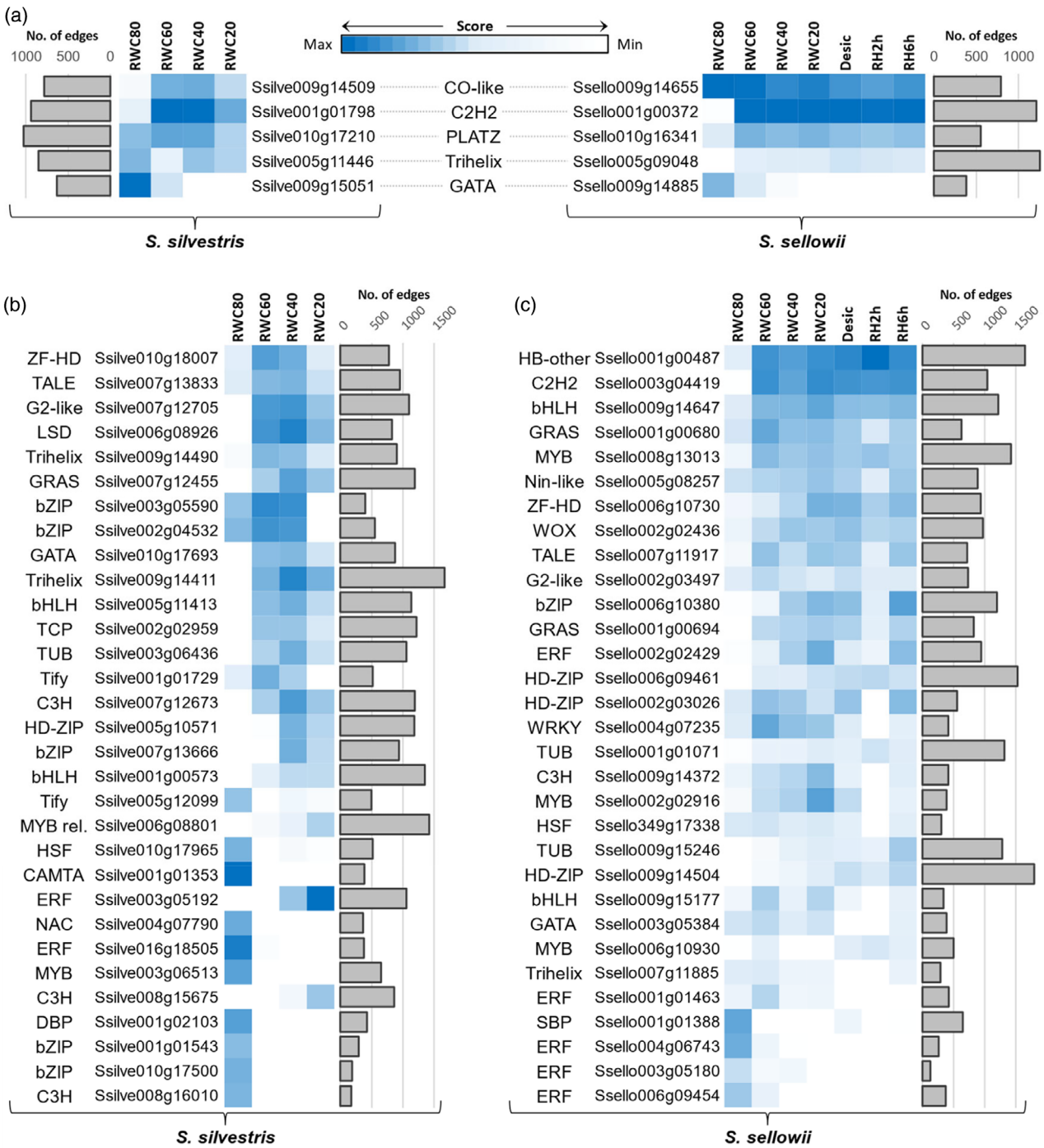

Figure 5. Candidate transcription factors (TFs) participating as key regulators of VDT in *Selaginella*.
(a) TFs identified as shared regulators (syntenic orthologs) in both *Selaginella* species during desiccation treatment.
(b) TFs identified as regulators only in the desiccation-sensitive *S. silvestris* during dehydration.
(c) Key regulators identified only in the desiccation-tolerant *S. sellowii* during dehydration and rehydration stages. Dehydration conditions expressed as different relative water contents (RWC), and recovery stage expressed as hours after rehydration (RH). Regulators were sorted in descending order by their average score across all conditions. The intensity of the blue boxes represents the TF's score, while the gray bars indicate the number of edges of each regulator.

downregulated clusters, whereas the desiccation-sensitive *S. silvestris* had six upregulated and three downregulated clusters. A functional enrichment analysis was performed to determine the type of processes associated with each cluster. For the desiccation-tolerant *S. sellowii*, the largest cluster corresponds to upregulated genes (cluster No. 2),

and it is mainly involved in abiotic stress responses, stomatal movement, redox response, and protection mechanisms (phospholipid metabolism, glutathione metabolic process, etc.). The next two largest clusters in *S. sellowii* (clusters No. 5 and 7) represent downregulated clusters highly enriched in morphogenesis, development, and cell cycle, as well as photosynthesis and modifications in photosynthetic apparatus. Similarly, the largest cluster in the desiccation-sensitive *S. silvestris* (cluster No. 5), which includes downregulated genes, was highly enriched in photosynthesis and modifications in the photosynthetic apparatus but in a lower proportion to morphogenesis, development, and cell cycle. The second largest cluster in *S. silvestris* (cluster No. 8), associated with upregulated genes, was barely enriched in VDT protection mechanisms. Figure S12 presents a summary of each cluster's general categories.

Comparative analyses using orthogroups showed important differences in gene expression patterns between the desiccation-tolerant *S. sellowii* and the desiccation-sensitive *S. silvestris*. For instance, large clusters containing upregulated genes in *S. sellowii*, such as clusters 2 and 3, were associated with VDT protection mechanisms. Interestingly, some homologous genes in the desiccation-sensitive species exhibited low transcript increases or an opposite expression pattern (Figure 6a). Specifically, these differences in gene expression include genes putatively involved in fatty acid biosynthesis, oxylipin biosynthetic process, regulation of stomatal closure, protein ubiquitination, glutathione metabolic process, and response to hydrogen peroxide, among others (Data S4). Similarly, some downregulated genes during water loss in the desiccation-tolerant species are induced in the desiccation-sensitive *S. silvestris*. Such genes with opposite patterns are involved in processes like tissue pattern formation, cell fate and differentiation, stomatal complex, and embryonic morphogenesis (Data S4).

DISCUSSION

The genetic potential for DT is present in nearly all vascular plants; however, in most plants, DT is limited to specific structures such as seeds, pollen, and spores (Ballesteros et al., 2020; Costa, Cooper, et al., 2017; Smolikova et al., 2020). Resurrection plants evolved the remarkable ability to activate desiccation protection mechanisms in their vegetative tissues (Figure 1d; Video S1). Although several recent omics studies have been reported, the molecular mechanisms underlying DT in resurrection plants are still poorly understood. One of the major problems is the complexity of resurrection genomes (e.g., polyploid species) and the need for more tools for genetic and functional genomics analysis. Compared to other resurrection lineages, *Selaginella* species possess relatively simple and small genomes (commonly diploid species with a maximum genome haploid size of around 182 Mb) (Baniaga et al., 2016). Although previous studies have reported high heterozygosity in *Selaginella* genomes (up to 2%) (Banks et al., 2011; VanBuren et al., 2018; Xu et al., 2018), the results of this study indicated a much lower heterozygosity value of $<$0.8% using clonally propagated *Selaginella* individuals. This starting plant material allowed the generation of genome assemblies with a higher proportion of conserved, single-copy genes and a more complete annotation than other available *Selaginella* genomes (Figure 2a). Our synteny comparison highlighted high gene collinearity at the chromosome level between the genomes of the desiccation-sensitive *S. silvestris* and the desiccation-tolerant *S. sellowii* (Figure 1b), and revealed that most of the genes involved in VDT are present in both species (Figure S4). The availability of high-quality chromosome-level genome assemblies and closely related species with contrasting abilities to survive desiccation will facilitate using *Selaginella* species as models for comparative analyses to identify genomic features and key responses for VDT.

A combined multi-omic approach, including transcriptomic, metabolomic, and lipidomic data, was carried out to identify differential responses and mechanisms between *Selaginella* species that could be associated with VDT. First, we analyzed the differences between these two *Selaginella* species under well-hydrated conditions. We found that the resurrection species *S. sellowii* appears to have a predisposition or preadaptation for VDT by transcriptional priming of stress-related genes (Figure 3). Genes participating in ABA signaling and defense response have high transcript levels and are significantly enriched in hydrated conditions in this species. For instance, genes participating in the lignin biosynthetic process are highly expressed in well-watered tissue of *S. sellowii*, but not in the desiccation-sensitive *S. silvestris* until the onset of water loss. Nevertheless, one of the most significant differences between *Selaginella* species was the accumulation of flavonoids in well-watered conditions of the desiccation-tolerant *S. sellowii*, whose level is maintained or even increased during water loss, indicating that accumulation of flavonoids is a constitutive strategy for VDT (Data S1). As expected from the accumulation of flavonoids, transcript levels of genes involved in flavonoid biosynthesis are high in the hydrated condition and maintained during the whole desiccation process in *S. sellowii* (Figure 3b,c). Moreover, our data show that specific genes, other than the ELIPs gene family, were expanded in the genome of the desiccation-tolerant species, such as those involved in flavonoid biosynthesis. Specifically, genes coding for chalcone synthase, a key enzyme for flavonoid biosynthesis, were expanded in the resurrection *S. sellowii* by tandem gene duplications (Figure 2d). This enzyme provides the starting material to produce distinct flavonoids, and it is

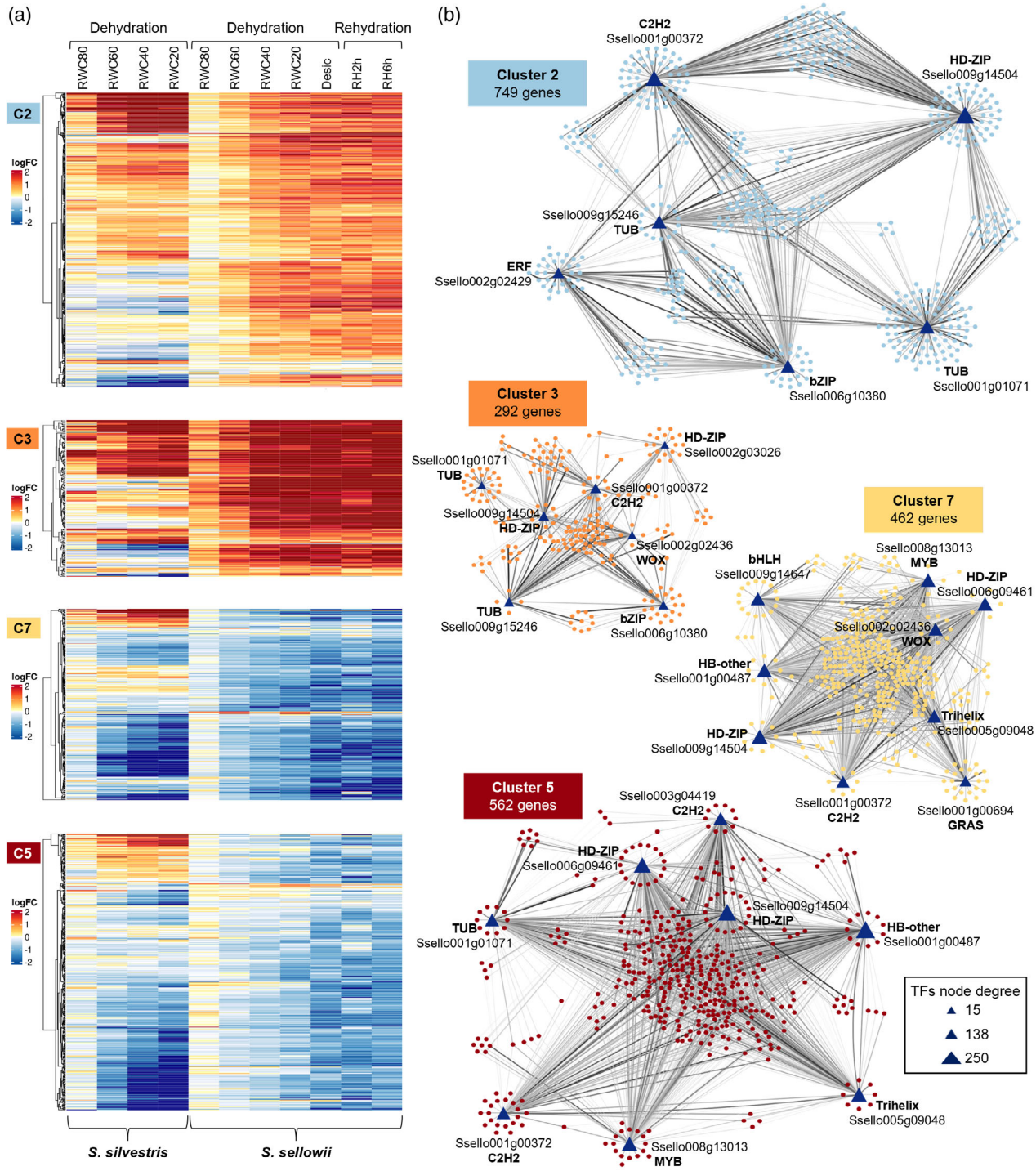

Figure 6. Gene expression differences between tolerant and sensitive *Selaginella* species in clusters controlling important VDT protection mechanisms.
(a) Heatmaps showing gene expression of the largest four clusters (cluster No. 2, 3, 5, and 7) in the desiccation-tolerant *S. sellowii* compared to the desiccation-sensitive *S. silvestris* using orthogroups.
(b) Representation of the regulatory networks associated with each cluster and the candidate TFs participating as regulators.

induced in response to stress conditions, including UV light stress (Dao et al., 2011). Flavonoids are important protective molecules against UV and high-light exposure (Ferreyra et al., 2021). Probably, *S. sellowii* evolved a constitutive accumulation of flavonoids as an adaptation to habitats with high solar radiation, where this species

usually grows to protect cells against oxidative stress as scavengers of reactive oxygen species (ROS) during desiccation. The resurrection relative *S. lepidophylla* exhibits a similar accumulation of high levels of flavonoids such as apigenin, luteolin, and naringenin in hydrated conditions (Yobi et al., 2013). Our data indicate apigenin-7-O-beta-D-glucoside, also known as apigetrin or cosmosiin, as the most abundant flavonoid in desiccation-tolerant *S. sellowii*. Apigetrin possesses antioxidant activity (Yin et al., 2008) and most likely participates as a ROS scavenger in *Selaginella* VDT. Resurrection species that keep their photosynthetic machinery during desiccation, such as *S. sellowii*, must exhibit efficient antioxidant systems to avoid cellular damage by the excess of ROS produced when the plant cannot assimilate all the electrons generated by the photosynthetic electron transfer chains. It has been suggested that resurrection plants can survive desiccation without damage if their antioxidant machinery remains functional (Kranner & Birtić, 2005). Therefore, antioxidant defense mechanisms to scavenge ROS constitute essential traits of desiccation-tolerant plants. Other antioxidant responses activated only in the desiccation-tolerant *S. sellowii* include the induction of glutathione synthesis (Figure 4). Metabolomic analyses confirmed that glutathione biosynthesis is activated below 40% RWC in *S. sellowii* and is at least ten times more abundant than in the desiccation-sensitive species (Figure S6). This antioxidant is accumulated during desiccation in several resurrection plants, and it has been proposed as one of the principal active compounds against ROS activity in other resurrection species such as *Sporobolus stapfianus* (Oliver et al., 2011) and *Myrothamnus flabellifolia* (Kranner et al., 2002).

In a previous study, we determined that the desiccation-sensitive *S. silvestris* begins to lose viability at 40% relative water content (RWC), and at 20% RWC, most of its tissue suffers irreversible damage (Alejo-Jacuinde et al., 2022). These points represent critical conditions during water loss in the desiccation-sensitive species. Most plants trigger leaf senescence programs under drought stress as a survival strategy (Munné-Bosch & Alegre, 2004). Under these critical conditions, the transcript levels of leaf senescence genes increased in the desiccation-sensitive *S. silvestris* at 20% RWC. In contrast, resurrection plants appear to have evolved strategies to suppress the drought-induced senescence response (Griffiths et al., 2014). Comparative genomic analysis indicated a significant contraction of certain senescence-related genes in the genomes of resurrection *Selaginella* species (Figure 2c). Our findings also suggest that *S. sellowii* likely employs additional strategies to avoid senescence. Both *Selaginella* species increased the abundance of transcripts related to lipid metabolism in response to water loss. However, the desiccation-tolerant species specifically induced genes participating in phospholipid metabolism (Figure 4). A change in the abundance of phospholipids in response to desiccation has been reported in other resurrection plants, but it has been associated with the structural stabilization of membranes (Gasulla et al., 2013; Quartacci et al., 2002). Major changes in lipid composition in response to water loss were detected in both *Selaginella* species, but more pronounced changes were observed in the desiccation-tolerant *S. sellowii*, including a significant increase in lysophospholipids of the LPE and LPC classes (Figure S7). Previous studies showed that exogenous application of LPE delays leaf senescence (Farag & Palta, 1993; Hong et al., 2009). Therefore, the increase in the abundance of LPE in the resurrection *S. sellowii* could play an important role in regulating the drought-induced senescence response. Lysophospholipids represent key components of plant signaling pathways and are produced by phospholipase A (PLA) (Cowan, 2006; Wang et al., 2012). Importantly, PLA genes were also expanded in the genomes of resurrection *Selaginella* species (Figure 2c), suggesting that several key differential responses between tolerant and sensitive species are associated with gene family rearrangements.

Most genes participating in the desiccation response in the resurrection *S. sellowii* belong to gene families present in both tolerant and sensitive *Selaginella* species (97% of the gene families including SDATs; Figure S4). Thus, there is a paramount interest in identifying the regulators controlling the expression of these genes in the vegetative tissue of desiccation-tolerant species. Analysis of regulatory networks allowed the identification of 36 TFs potentially participating as central regulators of VDT in *Selaginella* (Figure 5). This analysis showed that most of the TFs recruited for VDT in a resurrection species differ from the TFs used to activate the response to water loss in a desiccation-sensitive plant. Several studies have reported the induction of genes involved in seed maturation in vegetative tissues of resurrection plants (Chávez Montes et al., 2022; Costa, Artur, et al., 2017; VanBuren, 2017; VanBuren et al., 2017), suggesting that VDT likely evolved by rewiring seed DT pathways. Members of the denominated LAFL (LEC1, ABI3, FUS3, LEC2) network, which correspond to master regulators of seed maturation programs (Santos-Mendoza et al., 2008; Verma et al., 2022), were not identified as main regulators for VDT in the resurrection *S. sellowii*. A similar pattern was observed in *X. humilis*, in which LAFL orthologs are upregulated during seed maturation but not during its response to desiccation treatments (Lyall et al., 2020). However, homologs of some TFs acting downstream of the LAFL network were identified in our analyses. These TFs are involved in the acquisition of DT in *Arabidopsis thaliana* seeds (González-Morales et al., 2016), and they include homologs to the ERF8, ERF12, ERF23, TZF4/5, and PLATZ genes (Ssello001g01463,

Ssello002g02429, Ssello004g06743, Ssello006g09454, Ssello009g14372, and Ssello010g16341 respectively). In the desiccation-tolerant *S. sellowii*, these TFs are associated with genes involved in abiotic and biotic stress responses, ABA signaling, and immune response.

Drought stress severely affects photosynthesis, but resurrection plants have evolved mechanisms to recover photosynthetic activity after desiccation (Challabathula et al., 2016). Our analyses showed photosynthesis-related categories as one of the most enriched processes in *S. sellowii* regulatory network (Figure S8), indicating the importance of regulating photosynthesis during VDT. Although both *Selaginella* species display transcriptional repression of genes related to cell cycle, development, and morphogenesis during water stress, growth inhibition has a central role in the regulatory networks of the desiccation-tolerant *S. sellowii* (Figure S12). Generally, plant species adapted to environments with extreme conditions usually grow slowly, likely due to a strategy to ensure survival (Zhang et al., 2020). Resurrection plants grow slowly even in unstressed conditions with abundant resources; therefore, it can be hypothesized that their slow growth rate is an inherent consequence of VDT evolution. However, our results suggest that resurrection plants such as *S. sellowii* evolved a more efficient strategy by inhibiting growth during water loss compared to desiccation-sensitive species. Comparative analysis using orthogroups showed that sets of genes downregulated in the desiccation-tolerant *S. sellowii* are upregulated in its sensitive counterpart (Figure 6), such as those involved in processes of tissue pattern formation, regulation of cell differentiation, root development, and stomatal complex morphogenesis (Data S4). Such responses can represent an ultimate survival effort in response to water loss in the desiccation-sensitive *Selaginella* species. Rather than investing energy in tissue adaptation to water stress conditions, desiccation-tolerant *S. sellowii* could use its energetic resources for protection and damage repair mechanisms.

We show that the vegetative tissues of the desiccation-tolerant *S. sellowii* are transcriptionally primed for stress tolerance and more responsive to dehydration. We found that the accumulation of protective metabolites in unstressed conditions (i.e., flavonoid accumulation) seems to be an important component of the VDT mechanisms in resurrection *Selaginella* species. Our findings show that some key differences between tolerant and sensitive *Selaginella* species are associated with gene family rearrangements (e.g., phospholipase and senescence-related genes), suggesting that changes in gene dosage by family expansions and contractions had an important role in the evolution of VDT. Finally, analysis of regulatory networks revealed a central role for the downregulation of plant growth in *S. sellowii*, which is likely to redirect resources toward protection rather than growth. Apparently, the desiccation-tolerant species changed from a growth mode to a protection mode, redirecting its energetic metabolism to produce protective compounds and modifications to survive desiccation. These findings might lay the basis for the future genome engineering of crops adapted to extreme water conditions, regulating a trade-off between growth and protection mechanisms.

EXPERIMENTAL PROCEDURES

Plant material and desiccation treatments

The two *Selaginella* species were propagated by cuttings and maintained in a growth chamber at 22°C under a 16/8-h photoperiod. For the desiccation-tolerant *S. sellowii*, clonally propagated material was grown for more than a year to generate enough material for genome sequencing. The drying system and dehydration experiments were performed as described previously (Alejo-Jacuinde et al., 2022). Briefly, small plastic containers (140 mL) with a saturated solution of $MgCl_2$ (32%–33% RH) were used as desiccators. Explants with an approximate turgid weight of approximately 100 mg (3–4 explants) were used for desiccation experiments. Fully hydrated tissue (T_w; turgor weight after submerging explants in water for 24 h) were placed in the drying system and weighted at regular intervals (F_w) to determine water loss. Dry weight (D_w) was obtained after drying the tissue at 65°C for 48 h. The relative water content (RWC) was calculated:

$$\mathrm{RWC} = [(F_w - D_w)/(T_w - D_w)] \times 100. \quad (1)$$

Explants for the transcriptomic, metabolomic, and lipidomic analyses were collected at 100%, 80%, 60%, 40%, and 20% RWC for both *S. silvestris* and *S. sellowii*. Additionally, tissue was collected at the desiccated state and during rehydration (2 and 6 h) for transcriptomic analyses in the desiccation-tolerant *S. sellowii*. An initial fresh weight (turgid weight) of approximately 100 mg of plant tissue was used as the starting material for all samples in the transcriptomic, metabolomic, and lipidomic analyses. Explant drying rate and sampling time points are shown in Figure S1.

Nucleic acid extractions and sequencing

Tissue for nucleic acid extractions was flash-frozen in liquid nitrogen and stored at −80°C until used. A modified CTAB protocol with a sorbitol pre-wash step (Inglis et al., 2018) was used for extraction of high molecular weight DNA for PacBio and Illumina sequencing. Nuclei for Hi-C samples were isolated as described by Peterson et al. (1997). Nuclei crosslinking and the preparation of proximally ligated DNA were performed as described in the Arima-HiC 2.0 protocol (Arima Genomics). Hi-C scaffolding libraries were prepared using the Swift Accel NGS 2S Plus Kit following the manufacturer's instructions. RNA was extracted using the RNeasy Plant Mini Kit (Qiagen) according to the manufacturer's instructions. PacBio (Sequel system), Illumina (NovaSeq; paired-end 150 bp mode), and Hi-C sequencing were conducted by Novogene (Beijing, China).

Genome heterozygosity and assembly

Illumina reads were trimmed for quality and sequencing adapters using TrimGalore (v0.6.6; https://github.com/FelixKrueger/TrimGalore). Quality trimmed Illumina reads were used to generate histograms of the *k*-mer (21-mer) frequency distribution with Jellyfish (Marçais & Kingsford, 2011) (v2.3.0). Genome

heterozygosity was estimated with the webtool GenomeScope (Vurture et al., 2017) and the package findGSE (Sun et al., 2018) (v1.94). The final *Selaginella* genomes were generated using MaSuRCA (Zimin et al., 2017) (v3.4.2). The software BlobTools (Laetsch & Blaxter, 2017) (v1.1.1) was used to detect genome contamination. The raw PacBio and Illumina reads that mapped to the putative contaminant contigs were manually removed to generate a contamination-free MaSuRCA assembly for the species *S. sellowii*. The Purge Haplotigs (Roach et al., 2018) (v1.1.1) software was used to produce a primary haploid assembly for the species *S. silvestris*. Assemblies were polished using five iterations of Pilon (Walker et al., 2014) (v1.24) with Illumina data. Contigs were reordered and connected into scaffolds using Juicer (Durand et al., 2016) and 3D-DNA (Dudchenko et al., 2017) pipelines with Hi-C data. A detailed description of the genome assembly strategy for *Selaginella* species is shown in Method S1. Genome completeness was evaluated using BUSCO (Simão et al., 2015) (v5.4.3) with viridiplantae and eukaryota datasets (odb10). Chromosome circular maps were generated using Circos (Tang et al., 2008) (v0.69–9). For the comparative genomic analyses between *S. sellowii* and *S. silvestris* the MCScan algorithm was used to identify syntenic blocks (Tang et al., 2008). Orthology between *S. kraussiana*, *S. moellendorffii*, *S. lepidophylla*, *S. sellowii*, *S. silvestris*, and *S. tamariscina* was determined using OrthoFinder (Emms & Kelly, 2015) (v2.5.5). For the identification of gene family expansions and contractions the analysis was limited to phylogenetically close *Selaginella* species that differ in their ability to survive desiccation.

Structural and functional genome annotation

Selaginella genomes were annotated through three rounds of MAKER-P (Cantarel et al., 2008; Holt & Yandell, 2011a) (v3.01.03) using transcripts as EST evidence (RNA-seq libraries), the plants in the OrthoDB odb10 dataset as protein homology, and sequences obtained using RepeatModeler (v2.0.3) as repeats file. The second round used the maker gff3 file from the first round as input, a SNAP hmm file obtained from round 1 gene models, and the Augustus (Stanke et al., 2006) gene models from a BUSCO (Manni et al., 2021). The third round was run the same as the second round, using round 2 output files as inputs. Genome annotation completeness was evaluated using BUSCO (Simão et al., 2015) with eukaryota and viridiplantae datasets (odb10).

Genome functional annotation was produced using a modified version of the MAIZE-gamer pipeline (Wimalanathan et al., 2018). Annotations were assigned as the gene ontology (GO) annotations of the BLASTP reciprocal best hits versus Araport11 and UniProt Swiss-Prot proteins (including nine plant species), GO annotations from InterProScan (Blum et al., 2021) (v5.57–90.0), and PANNZER2 (Törönen et al., 2018) functional annotation webserver. A detailed description of the structural and functional genome annotation is described in Method S1.

Metabolomic and lipidomic analyses

The preparation of the polar and non-polar fractions (metabolomics and lipidomics analysis, respectively) are described in the Methods S1. These samples were injected into a reverse phase C18 column and separated using a chromatographic gradient composed of water with 0.1% formic acid as "mobile phase A" and methanol with 0.1% formic acid as the "mobile phase B" (MPB) for the polar fraction, whereas isopropyl alcohol 2 mM ammonium formate as the MPB for the non-polar fraction. The flow rate was set to 200 µL/min and the temperature at 50°C. For the polar phase, the gradient started with 5% of MPB for 4 min, then increased to 100% MPB in 13 min. This condition was maintained for 4 min and then set back to 5% MPB to re-equilibrate the system for 4 min. For the non-polar phase, the gradient started with 10% of MPB from 0 to 3 min, then MPB increased concentration to 50% from 3 to 7 min and further 50% to 100% MPB from 7 to 20 min. The 100% of MPB was kept constant for 6 min, then equilibrated to 10% from 26 to 30 min. Independent runs were completed for positive and negative detection modes with a scan range from 70 to 1700 m/z and a mass tolerance within 10 ppm with the mass resolution set at 120 K. The MS/MS spectra were acquired in data-dependent mode in a duty cycle of 1.5 s, and 30 K of resolution. Stepped high-energy collision dissociation was used as a fragmentation technique with N(CE) values of 25 and 30. The AGC target was set as standard with a Max IT of 54 ms, isolation window of 1.5 m/z, and a dynamic exclusion of 5 s. The raw files were uploaded to the Compound Discoverer software (v3.3; Thermo Sci.) and analyzed using a metabolomics pipeline. Metabolite identification was completed using mzCloud, KEGG, and BioCyc databases. For lipidomics, data analysis was performed using LipidSearch software (v5.5; Thermo Sci.) and LipidMaps database.

Gene expression, clustering, and gene regulatory networks

Expression levels of transcripts were quantified using kallisto (Bray et al., 2016) (v0.44). The package tximport (Soneson et al., 2016) was used to import the transcript level counts into R and summarized to gene level. Differential expression analyses were conducted using edgeR (Robinson et al., 2010). A cut-off of $|\log_2 FC| \geq 1$ and FDR <0.01 was used to identify SDATs. Functional enrichment analyses were conducted using topGO (Alexa & Rahnenführer, 2007) with Fisher's exact test and weight01 method. For comparative analyses between *Selaginella* species, expression was quantified in TPM, and the mean value across replicates was used to create $\log_2$ transformed expression-based heat maps. Differentially expressed genes were assigned to clusters using self-organizing maps (SOMs) with the kohonen R package (Wehrens & Buydens, 2007). For each *Selaginella* species, the previously identified SDATs were clustered using a 3 x 3 hexagonal SOM topology. A topGO (Alexa & Rahnenführer, 2007) analysis was performed to identify overrepresented GO categories for each cluster. Gene regulatory networks were inferred using the RegEnrich (Tao et al., 2022) package (v14.0); specific parameters, methods, and tools for network analyses are described in Method S1.

Statistical analysis

Statistical significance was calculated using software-integrated methods. A *P*-value of <0.05 was considered statistically significant for the overrepresented GO categories in the functional enrichment analyses.

AUTHOR CONTRIBUTIONS

GA-J, and LH-E conceived and designed the study; GA-J generated biological material for genome sequencing; GA-J, and RACM performed the genome assembly; LY-V generated the Hi-C data; RACM performed the structural and functional annotation; GA-J conducted comparative genomic analyses; CDGR performed the lipidomic, and metabolomic analyses; GA-J, and RACM, conducted the gene regulatory network analysis; GA-J, RACM, CDGR, LY-V, JS, and LH-E analyzed data; GA-J, JS, and LH-E wrote the

manuscript. All authors read and approved the final manuscript.

ACKNOWLEDGMENTS

This work was partially funded by the Governor University Research Initiative program (05-2018) from the State of Texas and the National Science Foundation (Award Number 2243690).

We are grateful to Araceli Oropeza-Aburto and Katia Gil-Vega for their technical assistance in establishing the protocol for nucleic acid isolation. We thank Héctor Rogelio Nájera González for providing suggestions for the metabolomic and lipidomic analyses. We thank Benjamin Perez Sanchez for his technical assistance and help in establishing the time-lapse video recording of the dehydration-rehydration process.

CONFLICT OF INTEREST

Authors declare that they have no conflict of interest.

DATA AVAILABILITY STATEMENT

Selaginella isolates are available by request from LH-E and GA-J. The raw DNA and RNA sequencing data are available at the NCBI under BioProject ID PRJNA1126682. Genome assemblies, gene models, structural and functional annotations generated in this study are available at https://www.depts.ttu.edu/igcast/Genomic/.

SUPPORTING INFORMATION

Additional Supporting Information may be found in the online version of this article.

Data S1. Metabolomic analyses of *S. sellowii* and *S. silvestris* during dehydration treatment.

Data S2. Lipidomic analyses of *S. sellowii* and *S. silvestris* during dehydration treatment.

Data S3. Fatty acids saturation and unsaturation analysis.

Data S4. Functional enrichment analysis of the differentially expressed genes in gene clusters.

Figure S1. Sampling timepoints for dehydration experiments.

Figure S2. k-mer frequency histograms showing *Selaginella* heterozygosity.

Figure S3. Completeness of *Selaginella* genome assemblies.

Figure S4. Homology analysis between *Selaginella* genomes.

Figure S5. Enriched categories in *S. sellowii* during the last stages of the desiccation process.

Figure S6. Gamma-glutamyl cycle pathway in *Selaginella*.

Figure S7. Changes in lipid composition after dehydration treatment in *Selaginella* species.

Figure S8. Enrichment analysis of the candidate regulator networks.

Figure S9. Gene regulatory network associated with key regulators and cluster analysis in the desiccation-tolerant *S. sellowii*.

Figure S10. Clusters and their expression profiles in the desiccation-sensitive *S. silvestris*.

Figure S11. Clusters and their expression profiles in the desiccation-tolerant *S. sellowii*.

Figure S12. GO biological terms associated with expression profile clusters of *Selaginella* species.

Figure S13. Gene expression and regulatory networks in *Selaginella*.

Method S1. Extended version of the experimental procedures used in the present study.

Table S1. *Arabidopsis thaliana* homologs of candidate regulators and their proposed biological function.

Video S1. Time-lapse recording showing the dehydration-rehydration process of *Selaginella* species with contrasting abilities to survive desiccation. Time-lapse photography of the dehydration treatment (first 24 hours) and rehydration process (first 6 hours) of *S. sellowii* (desiccation tolerant) and *S. silvestris* (desiccation sensitive). A saturated solution of $MgCl_2$ (32 – 33% RH) was used for the dehydration experiment.

REFERENCES

Alejo-Jacuinde, G. & **Herrera-Estrella, L.** (2022) Exploring the high variability of vegetative desiccation tolerance in Pteridophytes. *Plants*, **11**, 1222.

Alejo-Jacuinde, G., **Kean-Galeno, T.**, **Martínez-Gallardo, N.**, **Tejero-Díez, J.D.**, **Mehltreter, K.**, **Délano-Frier, J.P.** ***et al.*** (2022) Viability markers for determination of desiccation tolerance and critical stages during dehydration in Selaginella species. *Journal of Experimental Botany*, **73**, 3898–3912.

Alexa, A. & **Rahnenführer, J.** (2007) Gene set enrichment analysis with topGO. *Bioconductor Improv*, **27**, 1–26.

Alpert, P. & **Oliver, M.J.** (2002) Drying without dying. In: Black, M. & Pritchard, H.W. (Eds.) *Desiccation and survival in plants: drying without dying*. Wallingford: CABI, pp. 3–43.

Artur, M.A.S. & **Kajala, K.** (2021) Convergent evolution of gene regulatory networks underlying plant adaptations to dry environments. *Plant, Cell & Environment*, **44**, 3211–3222.

Ballesteros, D., **Pritchard, H.W.** & **Walters, C.** (2020) Dry architecture: towards the understanding of the variation of longevity in desiccation-tolerant germplasm. *Seed Science Research*, **30**, 142–155.

Baniaga, A.E., **Arrigo, N.** & **Barker, M.S.** (2016) The small nuclear genomes of Selaginella are associated with a low rate of genome size evolution. *Genome Biology and Evolution*, **8**, 1516–1525.

Banks, J.A., **Nishiyama, T.**, **Hasebe, M.**, **Bowman, J.L.**, **Gribskov, M.**, **dePamphilis, C.** ***et al.*** (2011) The Selaginella genome identifies genetic changes associated with the evolution of vascular plants. *Science*, **332**, 960–963.

Blum, M., **Chang, H.Y.**, **Chuguransky, S.**, **Grego, T.**, **Kandasaamy, S.**, **Mitchell, A.** ***et al.*** (2021) The InterPro protein families and domains database: 20 years on. *Nucleic Acids Research*, **49**, D344–D354.

Bray, N.L., **Pimentel, H.**, **Melsted, P.** & **Pachter, L.** (2016) Near-optimal probabilistic RNA-seq quantification. *Nature Biotechnology*, **34**, 525–527.

Cantarel, B.L., **Korf, I.**, **Robb, S.M.C.**, **Parra, G.**, **Ross, E.**, **Moore, B.** ***et al.*** (2008) MAKER: an easy-to-use annotation pipeline designed for emerging model organism genomes. *Genome Research*, **18**, 188–196.

Challabathula, D., **Puthur, J.T.** & **Bartels, D.** (2016) Surviving metabolic arrest: photosynthesis during desiccation and rehydration in resurrection plants. *Annals of the New York Academy of Sciences*, **1365**, 89–99.

Chávez Montes, R.A., **Haber, A.**, **Pardo, J.**, **Powell, R.F.**, **Divisetty, U.K.**, **Silva, A.T.** ***et al.*** (2022) A comparative genomics examination of desiccation tolerance and sensitivity in two sister grass species. *Proceedings of the National Academy of Sciences of the United States of America*, **119**, e2118886119.

Costa, M.-C.D., **Artur, M.A.S.**, **Maia, J.**, **Jonkheer, E.**, **Derks, M.F.L.**, **Nijveen, H.** ***et al.*** (2017) A footprint of desiccation tolerance in the genome of Xerophyta viscosa. *Nature Plants*, **3**, 17038.

Costa, M.C.D., **Cooper, K.**, **Hilhorst, H.W.M.** & **Farrant, J.M.** (2017) Orthodox seeds and resurrection plants: two of a kind? *Plant Physiology*, **175**, 589–599.

Cowan, A.K. (2006) Phospholipids as plant growth regulators. *Plant Growth Regulation*, **48**, 97–109.

Dao, T.T.H., **Linthorst, H.J.M.** & **Verpoorte, R.** (2011) Chalcone synthase and its functions in plant resistance. *Phytochemistry Reviews*, **10**, 397–412.

Dudchenko, O., **Batra, S.S.**, **Omer, A.D.**, **Nyquist, S.K.**, **Hoeger, M.**, **Durand, N.C.** ***et al.*** (2017) De novo assembly of the Aedes aegypti genome using hi-C yields chromosome-length scaffolds. *Science*, **356**, 92–95.

Durand, N.C., **Shamim, M.S.**, **Machol, I.**, **Rao, S.S.P.**, **Huntley, M.H.**, **Lander, E.S.** ***et al.*** (2016) Juicer provides a one-click system for analyzing loop-resolution hi-C experiments. *Cell Systems*, **3**, 95–98.

Emms, D.M. & **Kelly, S.** (2015) OrthoFinder: solving fundamental biases in whole genome comparisons dramatically improves orthogroup inference accuracy. *Genome Biology*, **16**, 157.

Farag, K.M. & **Palta, J.P.** (1993) Use of lysophosphatidylethanolamine, a natural lipid, to retard tomato leaf and fruit senescence. *Physiologia Plantarum*, **87**, 515–521.

Farrant, J.M., **Brandt, W.** & **Lindsey, G.G.** (2007) An overview of mechanisms of desiccation tolerance in selected angiosperm resurrection plants. *Plant Stress*, **1**, 72–84.

Ferreyra, M.L.F., **Serra, P.** & **Casati, P.** (2021) Recent advances on the roles of flavonoids as plant protective molecules after UV and high light exposure. *Physiologia Plantarum*, **173**, 736–749.

Gasulla, F., **Vom Dorp, K.**, **Dombrink, I.**, **Zähringer, U.**, **Gisch, N.**, **Dörmann, P.** ***et al.*** (2013) The role of lipid metabolism in the acquisition of desiccation tolerance in Craterostigma plantagineum: a comparative approach. *The Plant Journal*, **75**, 726–741.

Gechev, T., **Lyall, R.**, **Petrov, V.** & **Bartels, D.** (2021) Systems biology of resurrection plants. *Cellular and Molecular Life Sciences*, **78**, 6365–6394.

Giarola, V., **Hou, Q.** & **Bartels, D.** (2017) Angiosperm plant desiccation tolerance: hints from Transcriptomics and genome sequencing. *Trends in Plant Science*, **22**, 705–717.

González-Morales, S.I., **Chávez-Montes, R.A.**, **Hayano-Kanashiro, C.**, **Alejo-Jacuinde, G.**, **Rico-Cambron, T.Y.**, **de Folter, S.** ***et al.*** (2016) Regulatory network analysis reveals novel regulators of seed desiccation tolerance in *Arabidopsis thaliana*. *Proceedings of the National Academy of Sciences*, **113**, E5232–E5241.

Griffiths, C.A., **Gaff, D.F.** & **Neale, A.D.** (2014) Drying without senescence in resurrection plants. *Frontiers in Plant Science*, **5**, 36.

Gupta, A., **Rico-Medina, A.** & **Caño-Delgado, A.I.** (2020) The physiology of plant responses to drought. *Science*, **368**, 266–269.

Hilhorst, H.W.M., **Costa, M.-C.D.** & **Farrant, J.M.** (2018) A footprint of plant desiccation tolerance. Does it exist? *Molecular Plant*, **11**, 1003–1005.

Holt, C. & **Yandell, M.** (2011a) MAKER2: an annotation pipeline and genome-database management tool for second-generation genome projects. *BMC Bioinformatics*, **12**, 1–14.

Hong, J.H., **Chung, G.H.** & **Cowan, A.K.** (2009) Delayed leaf senescence by exogenous lyso-phosphatidylethanolamine: towards a mechanism of action. *Plant Physiology and Biochemistry*, **47**, 526–534.

Inglis, P.W., **Pappas, M.C.R.**, **Resende, L.V.** & **Grattapaglia, D.** (2018) Fast and inexpensive protocols for consistent extraction of high quality DNA and RNA from challenging plant and fungal samples for high-throughput SNP genotyping and sequencing applications. *PLoS One*, **13**, e0206085.

Korotkevich, G., **Sukhov, V.**, **Budin, N.**, **Shpak, B.**, **Artyomov, M.N.** & **Sergushichev, A.** (2021) Fast gene set enrichment analysis. *bioRxiv*: 060012.

Kranner, I., **Beckett, R.P.**, **Wornik, S.**, **Zorn, M.** & **Pfeifhofer, H.W.** (2002) Revival of a resurrection plant correlates with its antioxidant status. *The Plant Journal*, **31**, 13–24.

Kranner, I. & **Birtić, S.** (2005) A modulating role for antioxidants in desiccation tolerance. *Integrative and Comparative Biology*, **45**, 734–740.

Laetsch, D.R. & **Blaxter, M.L.** (2017) BlobTools: interrogation of genome assemblies. *F1000Research*, **6**, 1287.

Lyall, R., **Schlebusch, S.A.**, **Proctor, J.**, **Prag, M.**, **Hussey, S.G.**, **Ingle, R.A.** ***et al.*** (2020) Vegetative desiccation tolerance in the resurrection plant *Xerophyta humilis* has not evolved through reactivation of the seed canonical LAFL regulatory network. *The Plant Journal*, **101**, 1349–1367.

Manni, M., **Berkeley, M.R.**, **Seppey, M.**, **Simão, F.A.** & **Zdobnov, E.M.** (2021) BUSCO update: novel and streamlined workflows along with broader and deeper phylogenetic coverage for scoring of eukaryotic, prokaryotic, and viral genomes. *Molecular Biology and Evolution*, **38**, 4647–4654.

Marçais, G. & **Kingsford, C.** (2011) A fast, lock-free approach for efficient parallel counting of occurrences of k-mers. *Bioinformatics*, **27**, 764–770.

Marks, R.A., **Farrant, J.M.**, **Nicholas McLetchie, D.** & **VanBuren, R.** (2021) Unexplored dimensions of variability in vegetative desiccation tolerance. *American Journal of Botany*, **108**, 346–358.

Munné-Bosch, S. & **Alegre, L.** (2004) Die and let live: leaf senescence contributes to plant survival under drought stress. *Functional Plant Biology*, **31**, 203–216.

Oliver, M.J., **Farrant, J.M.**, **Hilhorst, H.W.M.**, **Mundree, S.**, **Williams, B.** & **Bewley, J.D.** (2020) Desiccation tolerance: avoiding cellular damage during drying and rehydration. *Annual Review of Plant Biology*, **71**, 435–460.

Oliver, M.J., **Guo, L.**, **Alexander, D.C.**, **Ryals, J.A.**, **Wone, B.W.M.** & **Cushman, J.C.** (2011) A sister group contrast using untargeted global Metabolomic analysis delineates the biochemical regulation underlying desiccation tolerance in *Sporobolus stapfianus*. *The Plant Cell*, **23**, 1231–1248.

Oliver, M.J., **Tuba, Z.** & **Mishler, B.D.** (2000) The evolution of vegetative desiccation tolerance in land plants. *Plant Ecology*, **151**, 85–100.

Osakabe, Y., **Osakabe, K.**, **Shinozaki, K.** & **Tran, L.S.P.** (2014) Response of plants to water stress. *Frontiers in Plant Science*, **5**, 86.

Peterson, D.G., **Boehm, K.S.** & **Stack, S.M.** (1997) Isolation of milligram quantities of nuclear DNA from tomato (Lycopersicon esculentum), a plant containing high levels of polyphenolic compounds. *Plant Molecular Biology Reporter*, **15**, 148–153.

Proctor, M.C.F., **Oliver, M.J.**, **Wood, A.J.**, **Alpert, P.**, **Stark, L.R.**, **Cleavitt, N.L.** ***et al.*** (2007) Desiccation-tolerance in bryophytes: a review. *The Bryologist*, **110**, 595–621.

Quartacci, M.F., **Glišić, O.**, **Stevanović, B.** & **Navari-Izzo, F.** (2002) Plasma membrane lipids in the resurrection plant Ramonda serbica following dehydration and rehydration. *Journal of Experimental Botany*, **53**, 2159–2166.

Roach, M.J., **Schmidt, S.A.** & **Borneman, A.R.** (2018) Purge Haplotigs: allelic contig reassignment for third-gen diploid genome assemblies. *BMC Bioinformatics*, **19**, 1–10.

Robinson, M.D., **McCarthy, D.J.** & **Smyth, G.K.** (2010) edgeR: a Bioconductor package for differential expression analysis of digital gene expression data. *Bioinformatics*, **26**, 139–140.

Santos-Mendoza, M., **Dubreucq, B.**, **Baud, S.**, **Parcy, F.**, **Caboche, M.** & **Lepiniec, L.** (2008) Deciphering gene regulatory networks that control seed development and maturation in Arabidopsis. *The Plant Journal*, **54**, 608–620.

Simão, F.A., **Waterhouse, R.M.**, **Ioannidis, P.**, **Kriventseva, E.V.** & **Zdobnov, E.M.** (2015) BUSCO: assessing genome assembly and annotation completeness with single-copy orthologs. *Bioinformatics (Oxford, England)*, **31**, 3210–3212.

Smolikova, G., **Leonova, T.**, **Vashurina, N.**, **Frolov, A.** & **Medvedev, S.** (2020) Desiccation tolerance as the basis of long-term seed viability. *International Journal of Molecular Sciences*, **22**, 101.

Soneson, C., **Love, M.I.** & **Robinson, M.D.** (2016) Differential analyses for RNA-seq: transcript-level estimates improve gene-level inferences. *F1000Research*, **4**, 1521.

Stanke, M., **Schöffmann, O.**, **Morgenstern, B.** & **Waack, S.** (2006) Gene prediction in eukaryotes with a generalized hidden Markov model that uses hints from external sources. *BMC Bioinformatics*, **7**, 1–11.

Sun, H., **Ding, J.**, **Piednoël, M.** & **Schneeberger, K.** (2018) findGSE: estimating genome size variation within human and Arabidopsis using k-mer frequencies. *Bioinformatics*, **34**, 550–557.

Tang, H., **Bowers, J.E.**, **Wang, X.**, **Ming, R.**, **Alam, M.** & **Paterson, A.H.** (2008) Synteny and collinearity in plant genomes. *Science*, **320**, 486–488.

Tao, W., **Radstake, T.R.D.J.** & **Pandit, A.** (2022) RegEnrich gene regulator enrichment analysis reveals a key role of the ETS transcription factor family in interferon signaling. *Communications Biology*, **5**, 1–12.

Törönen, P., **Medlar, A.** & **Holm, L.** (2018) PANNZER2: a rapid functional annotation web server. *Nucleic Acids Research*, **46**, W84–W88.

VanBuren, R. (2017) Desiccation tolerance: seedy origins of resurrection. *Nature Plants*, **3**, 17046.

VanBuren, R., **Pardo, J.**, **Man Wai, C.**, **Evans, S.** & **Bartels, D.** (2019) Massive tandem proliferation of ELIPs supports convergent evolution of desiccation tolerance across land plants. *Plant Physiology*, **179**, 1040–1049.

VanBuren, R., **Wai, C.M.**, **Ou, S.**, **Pardo, J.**, **Bryant, D.**, **Jiang, N.** ***et al.*** (2018) Extreme haplotype variation in the desiccation-tolerant clubmoss Selaginella lepidophylla. *Nature Communications*, **9**, 13.

VanBuren, R., **Wai, C.M.**, **Zhang, Q.**, **Song, X.**, **Edger, P.P.**, **Bryant, D.** ***et al.*** (2017) Seed desiccation mechanisms co-opted for vegetative desiccation in the resurrection grass Oropetium thomaeum. *Plant, Cell & Environment*, **40**, 2292–2306.

Verma, S., **Attuluri, V.P.S.** & **Robert, H.S.** (2022) Transcriptional control of Arabidopsis seed development. *Planta*, **255**, 1–19.

Vurture, G.W., **Sedlazeck, F.J.**, **Nattestad, M.**, **Underwood, C.J.**, **Fang, H.**, **Gurtowski, J.** ***et al.*** (2017) GenomeScope: Fast reference-free genome profiling from short reads. *Bioinformatics*, **33**, 2202–2204.

Walker, B.J., **Abeel, T.**, **Shea, T.**, **Priest, M.**, **Abouelliel, A.**, **Sakthikumar, S.** ***et al.*** (2014) Pilon: an integrated tool for comprehensive microbial variant detection and genome assembly improvement. *PLoS One*, **9**, 112963.

Wang, G., **Ryu, S.** & **Wang, X.** (2012) Plant phospholipases: an overview. *Methods in Molecular Biology*, **861**, 123–137.

Wehrens, R. & **Buydens, L.M.C.** (2007) Self-and super-organizing maps in R: the kohonen package. *Journal of Statistical Software*, **21**, 1–19.

Wimalanathan, K., **Friedberg, I.**, **Andorf, C.M.** & **Lawrence-Dill, C.J.** (2018) Maize GO annotation—methods, evaluation, and review (maize-GAMER). *Plant Direct*, **2**, e00052.

Xu, Z., **Xin, T.**, **Bartels, D.**, **Li, Y.**, **Gu, W.**, **Yao, H.** ***et al.*** (2018) Genome analysis of the ancient Tracheophyte Selaginella tamariscina reveals evolutionary features relevant to the Acquisition of Desiccation Tolerance. *Molecular Plant*, **11**, 983–994.

Yin, J., **Si, C.L.** & **Wang, M.H.** (2008) Antioxidant activity of flavonoids and their glucosides from Sonchus oleraceus L. *Journal of Applied Biological Chemistry*, **51**, 57–60.

Yobi, A., **Wone, B.W.M.**, **Xu, W.**, **Alexander, D.C.**, **Guo, L.**, **Ryals, J.A.** ***et al.*** (2013) Metabolomic profiling in Selaginella lepidophylla at various hydration states provides new insights into the mechanistic basis of desiccation tolerance. *Molecular Plant*, **6**, 369–385.

Zhang, H., **Zhao, Y.** & **Zhu, J.K.** (2020) Thriving under stress: how plants balance growth and the stress response. *Developmental Cell*, **55**, 529–543.

Zimin, A.V., **Puiu, D.**, **Luo, M.C.**, **Zhu, T.**, **Koren, S.**, **Marçais, G.** ***et al.*** (2017) Hybrid assembly of the large and highly repetitive genome of Aegilops tauschii, a progenitor of bread wheat, with the MaSuRCA mega-reads algorithm. *Genome Research*, **27**, 787–792.